Article

SN 2017fzw: A fast-expanding type Ia supernova with transitional features

Jia-Yu Huang[1,2], Yang-Yang Li [1,2], Xiang-Yun Zeng [1,2,*], Sheng Zheng [1,2,*], Sarah A. Bird [1,2], Ju-jia Zhang [3,4,5], Ali Esamdin [6], Abdusamatjan Iskandar [6,7], K. Azaleee Bostroem [8,9], Shu-Guang Zeng [1,2], Yan-Shan Xiao [1,2], Yao Huang [1,2], D. Andrew Howell [8,9], Curtis McCully [8,9], Wen-Xiong Li [10], Tian-Meng Zhang [11], Li-Fan Wang [12] and Lei Hu[13]

1 Center for Astronomy and Space Sciences, China Three Gorges University, Yichang 443000, People's Republic of China
2 College of Science, China Three Gorges University, Yichang 443000, People's Republic of China
3 Yunnan Astronomical Observatories, Chinese Academy of Sciences, Kunming 650216, People's Republic of China
4 Key Laboratory for the Structure and Evolution of Celestial Objects, Chinese Academy of Sciences, Kunming 650216, People's Republic of China
5 Center for Astronomical Mega-Science, Chinese Academy of Sciences, 20A Datun Road, Chaoyang District, Beijing 100012, People's Republic of China
6 Xinjiang Astronomical Observatory, Chinese Academy of Sciences, Urumqi, Xinjiang 830011, People's Republic of China
7 School of Astronomy and Space Science, University of Chinese Academy of Sciences, Beijing 100049, People's Republic of China
8 Department of Physics, University of California, Santa Barbara, CA 93106-9530, USA
9 Las Cumbres Observatory, 6740 Cortona Drive Suite 102, Goleta, CA 93117-5575, USA
10 The School of Physics and Astronomy, Tel Aviv University, Tel Aviv 69978, Israel
11 Key Laboratory of Optical Astronomy, National Astronomical Observatories, Chinese Academy of Sciences, Beijing 100012, People's Republic of China
12 George P. and Cynthia Woods Mitchell Institute for Fundamental Physics & Astronomy, Texas A&M University, Department of Physics and Astronomy, 4242 TAMU, College Station, TX 77843, USA
13 Purple Mountain Observatory, Nanjing 210023, People's Republic of China
* Correspondence: xyzeng2018@ctgu.edu.cn, zsh@ctgu.edu.cn

Abstract: In this study, we analyzed the optical observations of a subluminous Type Ia supernova (SN Ia) 2017fzw, which exhibited high photospheric velocity (HV) at B-band maximum light. The absolute B-band peak magnitude was determined to be $M^B_{max} = -17.77 \pm 0.10$ mag, similar to 91bg-like SNe Ia. The decline rate of the B-band light curve was estimated to be $\Delta m_{15}(B) = 1.60 \pm 0.06$ mag. The spectra of SN 2017fzw were similar to those of 91bg-like SNe Ia, with prominent Ti II and Si II λ5972 features at early phases, gradually transitioning to spectra resembling normal (mainly HV subclass) SNe Ia at later phases, with a stronger Ca II NIR feature. Notably, SN 2017fzw exhibited spectral evolution features similar to those of HV SNe Ia at all phases, with a maximum-light Si II λ6355 velocity of $13,786 \pm 414$ km s^{-1} and a stonger Ca II NIR feature. Based on these findings, we classify SN 2017fzw as a transitional object with properties of both normal and 91bg-like SNe Ia, providing support for the hypothesis of a continuous distribution of supernovae between these two groups.

Keywords: supernovae: general; supernovae: individual: SN 2017fzw; transitional supernovae

1. Introduction

Type Ia supernovae (SNe Ia) are highly valued cosmological distance indicators [1] that have played a pivotal role in discovering the accelerating expansion of the universe [2] due to their uniform light curves and high luminosities. These supernovae are widely believed to arise from carbon-oxygen white dwarfs (WDs) experiencing explosive thermonuclear runaways [3]. Typically, their close-binary companion star is considered a non-degenerate object, known as the single-degenerate scenario (SD) [4,5], or another WD, known as the double-degenerate scenario (DD) [6]. Observations support both the SD and DD scenarios, which are both used to explain the observed diversity among SNe Ia [7,8].

The majority of SNe Ia ($\sim$ 70%) are classified as Branch normal groups, which exhibit relatively uniform photometric and spectroscopic evolution [9,10]. The remaining SNe

 doi:10.20944/preprints202305.1256.v1

Ia are grouped into various subclasses based on differences in their photometric and spectroscopic evolution compared to normal SNe Ia. For instance, the overluminous SN 1991T-like subclass is characterized by broad light curves, relatively weak Si II/S II and obvious Fe II/Fe III absorption features around the maximum light [11–13]. On the other hand, the subluminous SN 1991bg-like subgroup, such as SN 1999by [14], display a rapid decline rate in their light curves and strong absorption features of intermediate-mass elements (IMEs) [15,16]. Approximately $15-20\%$ of all SNe Ia belong to the rapid decliner class, accompanied by low peak luminosity in most cases [17–19]. Moreover, the rapid decliner class has a single I-band maximum delayed a few days with regard to the B-band maximum. For the 91bg-like group, the above behaviour is mainly due to their lower mass of ^{56}Ni [20,21]. Transitional SNe Ia have photometric and spectroscopic properties between normal and 91bg-like [22]. These transitional SNe Ia appear with a frequency as high as 91bg-like SNe Ia, such as SNe 1986G [23], 2011iv [24], and 2012ij [25].

Understanding the origin of transitional SNe Ia is crucial to gain insights into their properties lying between normal and 91bg-like SNe Ia. The identification of transitional SNe with a continuous distribution of observed properties supports the theory that normal and 91bg-like SNe share a common origin [26]. Transitional SNe Ia are characterized by a large light curve shape parameter ($\Delta m_{15}(B)$, the decline rate in B-band light curve over 15 days after the peak, [27,28]) and low luminosity, which are similar to 91bg-like SNe [24,26]. However, their near-infrared (NIR) light curves resemble those of normal SNe Ia that exhibit two maxima [24,29]. Spectroscopically, transitional SNe Ia show similarities to both normal and 91bg-like SNe Ia, which demonstrates their intermediate properties. Previous studies have reported that the range of the Phillips parameter for transitional groups is typically $1.5-1.8$ mag [19,30,31]. However, it is important to note that some SNe Ia beyond this range are also classified as transitional SNe, while some SNe Ia within this range do not exhibit any clear intermediate properties [20,32].

In this paper, we report on the photometric and spectroscopic observations of SN 2017fzw, which exhibits characteristics of a transitional SN Ia however with lower luminosity and high velocity (HV). In Section 2, we provide a detailed description of the observations and data reduction process. In Section 3, we present the optical light curves, color curves, estimation of reddening, and quasi-bolometric light curves of SN 2017fzw. In Section 4, we predict its mean spectral sequences and compare the spectral evolution with other SNe Ia. We discuss our findings in Section 5 and present our conclusions in Section 6.

2. Observations and Data Reduction

SN 2017fzw was first detected on August 9, 2017, at 0.41-m PROMPT-5 telescope, located at Cerro Tololo Inter-American Observatory (CTIO) during the Distance Less Than 40Mpc survey (DLT40) conducted by Tartaglia et al. (2018) [33]. Its coordinates were measured to be $\alpha = 06^{\rm h}21^{\rm m}34^{\rm s}.820$ and $\delta = -27^{\circ}12^{'}53^{''}.57$ (J2000), and its initial clear-filtered magnitude (AB) was recorded as approximately 17.17 mag [34,35]. Hosseinzadeh et al. (2017) [36] conducted a subsequent spectroscopic study, which identified SN 2017fzw as a 91bg-like SN Ia and determined its host galaxy to be NGC 2217 at a redshift of $z = 0.0054$. This corresponds to a distance modulus (μ) of $\mu = 31.66 \pm 0.15$ mag, or a distance of 21.45 Mpc (taking into account only the Virgo Infall) with an assumed Hubble constant of 67.8 km s^{-1} Mpc^{-1} [37,38]. 2017fzw is located approximately 100″away from the center of its host galaxy. Figure 1 displays the finder chart of SN 2017fzw.

Preprints (www.preprints.org) | NOT PEER-REVIEWED | Posted: 17 May 2023 doi:10.20944/preprints202305.1256.v1

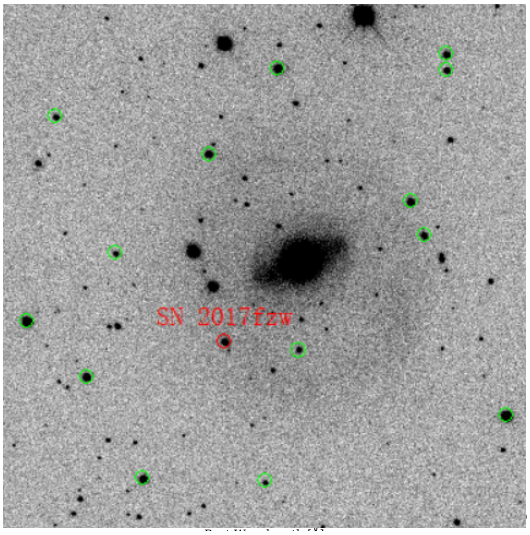

Figure 1. SN 2017fzw (red circle) and a local sequence of standard stars (green circles) in the field of NGC 2217 (*i*-band image, obtained by LCO on 07 September 2017 UT).

The optical photometry ($BVgri$) of SN 2017fzw was mainly collected by the Swope 1-m telescopes of Las Cumbres Observatory (LCO) [39,40] network for the Global Surpernova Project [41]. The data of LCO was reduced using `lcogtsnpipe` [42] and a `PyRAF`-based pipeline. The instrumental magnitudes of LCO are calibrated relative to Landolt (1992) [43] (BV) and Smith et al. (2002) [44] (gri) standard stars observed over multiple photometric nights, which are detailedly introduced by Krisciunas et al. (2017) [45] and Phillips et al. (2019) [46]. Ultraviolet (UV) and optical observations of this SN were also observed with the *Neil Gehrels Swift Observatory* (*Swift*) [47] in six bands, including $UVW1$, $UVW2$, $UVM2$, U, B and V filters [48]. The $UVM2$-band data could be ignored due to only four observations. According to the zero points of Breeveld et al. (2011) [49] in the Vega magnitudes, we obtained the *Swift* UV/optical light curves using the data-reduction pipeline of the *Swift* UV/optical Supernova Archive (SOUSA) [50]. We measured the source counts using a $3''$ aperture and corrected by an average point-spread function. Thus, the final flux-calibrated LCO and *Swift* light curves of SN 2017fzw are listed in Table A1, and shown in Figure 2.

After the discovery, optical observations were conducted using FLOYDS spectrographs mounted on the 2-m Faulkes Telescope North and South of the LCO [40,51], which are from the Global Supernova Project [41]. A total of 11 low-resolution optical spectra of this SN was obtained between -9 to $+168$ days. The spectral flux of SN 2017fzw are calibrated by standard stars observed with a comparable air mass as the SN on the same night. The LCO extinction curves and telluric correction are utilized to correct for the effects of atmospheric extinction and telluric absorption lines in the spectral data of SN 2017fzw.

3. Photometric Properties

3.1. Optical Light Curves and Time of First Light

Figure 2 shows the UV/optical light curves of SN 2017fzw. These light curves have a nearly daily cadence from about -10 to $+125$ days relative to B-band maximum light. Like normal SNe Ia, the r/i-band light curves of SN 2017fzw clearly show a shoulder/secondary maximum, and its light curve peak reached slightly earlier in i-band relative to B-band. These multi-band light curves were fit by `SuperNovae` in the object oriented Python code `SNooPy2` [52,53] to determine the time of B-band maximum light and other important light curve parameters, as shown in the left panel of Figure 3. We found that SN 2017fzw reached the B-band maximum light ($T_{max}(B)$) on MJD 57987.90 ± 0.35, corresponding to a peak magnitude of $B_{max} = 14.08 \pm 0.02$ mag and a decline rate $\Delta m_{15}(B) = 1.60 \pm 0.06$ mag estimated in the rest frame of this SN.

Preprints (www.preprints.org) | NOT PEER-REVIEWED | Posted: 17 May 2023 doi:10.20944/preprints202305.1256.v1

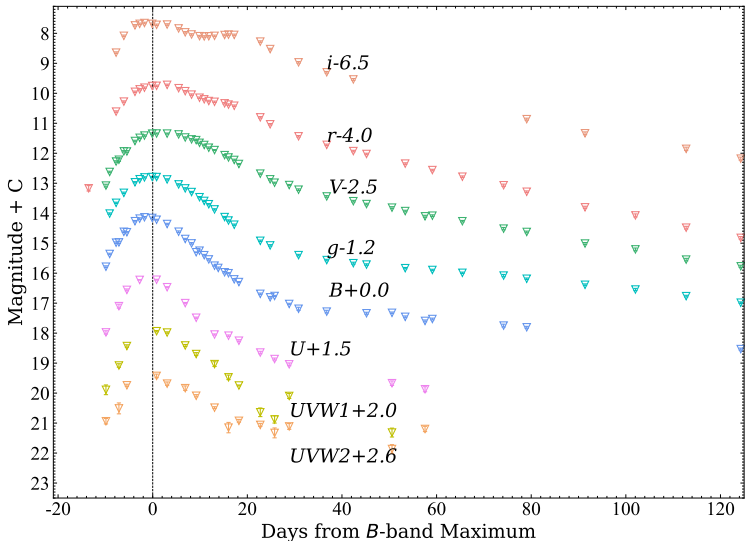

Figure 2. UV and optical (*UBVgri*) light curves of SN 2017fzw obtained by *Swift* and LCO. The vertical dashed line indicates its *B*-band maximum, and the light curves have been shifted vertically for clarity.

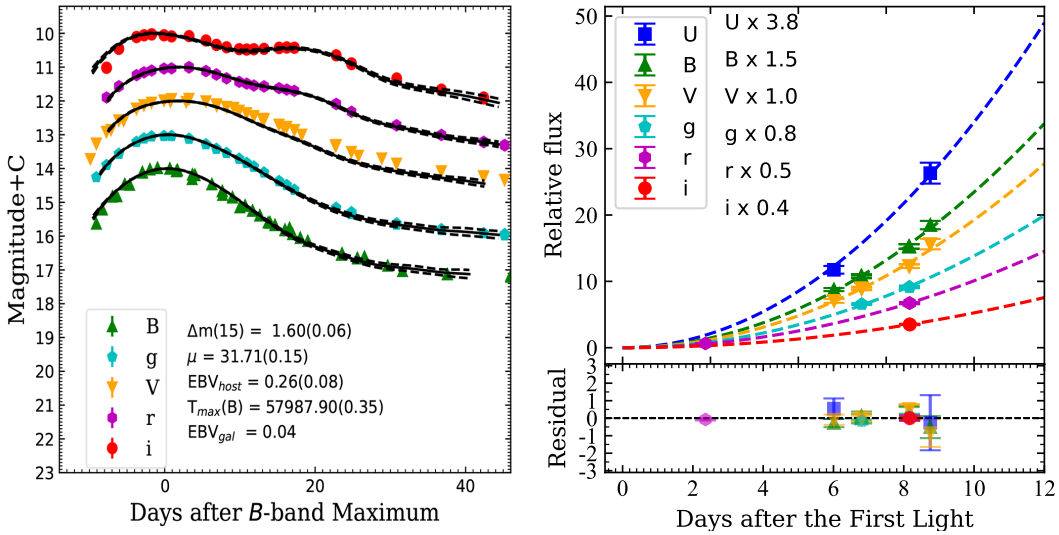

Figure 3. Left panel: best-fit light curve model (solid black lines) from `SNooPy2` [52,53] for SN 2017fzw. The dashed black lines indicate the 1-σ uncertainty (in many cases smaller than the line width) with respect to the best-fit light curve templates, and the light curves have been shifted vertically for clarity. Right panel: ideal fireball model [54] fits (dashed lines) to the multi-band early light curves of SN 2017fzw (markers with error vars) during the $\sim$ 7 days before the *B*-band maximum. The bottom panel displays the residual of the best-fit curves, and the horizontal black dashed line represents zero residual.

The time of first light (FLT) was estimated as MJD 57972.00 $\pm$ 0.24 by fitting the early multi-band light curves of SN 2017fzw during the $\sim$ 7 days before the *B*-band maximum with the ideal expanding fireball model [54], as shown in the right panel of Figure 3. Thus, its rise time is given as 15.9 $\pm$ 0.4 days, which is comparable to the average value of normal SNe Ia (i.e., 16.0 days, [55]) and also close to the upper limit value of 91bg-like SNe Ia ($\sim 13-15$ days, [20]). The basic photometric parameters of this SN are listed in Table 1, which are consistent with results of Graham et al. (2022) [56] within the uncertainties. For the following discussions, the phases are all given in reference to the *B*-band maximum of SN 2017fzw.

Preprints (www.preprints.org) | NOT PEER-REVIEWED | Posted: 17 May 2023 doi:10.20944/preprints202305.1256.v1

Table 1. The photometric and spectroscopic parameters of SN 2017fzw.

Parameter	Value
B_{max}	14.08 ± 0.02 mag
M^B_{max}	-17.77 ± 0.10 mag
$\Delta m_{15}(B)$	1.60 ± 0.06 mag
S_{BV}	0.63 ± 0.04
$T_{max}(B)$	MJD 57987.90 ± 0.35
FLT	MJD 57972.00 ± 0.24
Rise Time	15.9 ± 0.4 days
μ	33.71 ± 0.15 mag
Redshift	0.0054
v	$13,786 \pm 414$ km s^{-1}
M_{Ni}	0.18 ± 0.03 M$_\odot$

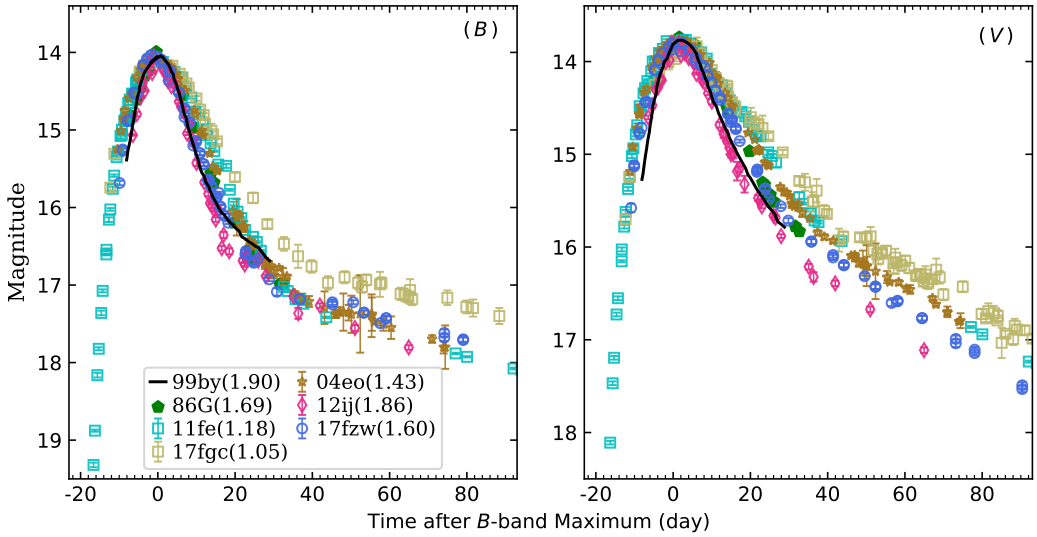

Figure 4. BV-band light curves of SN 2017fzw from LCO, compared with SNe 1999by (91bg-like subgroup), 2011fe, 2017fgc (normal subgroup), 2004eo, 1986G, and 2012ij (transitional subgroup). All light curves of comparison SNe Ia have been shifted to match SN 2017fzw in peak magnitudes.

In Figure 4, we compare the BV-band light curves of SN 2017fzw with those of some normal and subluminous SNe Ia, including SNe 1986G [23,28,57], 1999by [14,58], 2004eo [59], 2011fe [60], 2012ij [25], and 2017fgc [61]. One can see that the light curves of SN 2017fzw like other transitional SNe Ia are all similar to those of SN 1999by in terms of their morphology. Especially, the light curve of SN 2017fzw in V-band shows the strongest resemblance to that of transitional SN 1986G having similar $\Delta m_{15}(B)$.

3.2. Reddening and Color Curves

According to the NASA/IPAC Extragalactic Database (NED) [38], the Galactic extinction toward SN 2017fzw is $A_B^{Gal} = 0.16$ [62]. Since the Na I D absorption feature was nondetectable in this SN spectra, the reddening of the host galaxy was assumed to be negligible. Fitting the multi-band light curves of SN 2017fzw with `SNooPy2` estimate its μ as 31.71 ± 0.15 mag (see the left panel of Figure 3). Taking μ of its host galaxy as 31.66 ± 0.15 mag into account, we adopt their average value of $\mu = 31.69 \pm 0.11$ mag and an extinction law $R_V = 3.1$ [63] in the following analysis. Then, the B-band absolute peak magnitude of SN 2017fzw was deduced as $M^B_{max} = -17.77 \pm 0.10$ mag, which is comparable to that of 91bg-like SNe Ia (about -16.5 to -17.7 mag [64]).

In Figure 5, we compare the SN 2017fzw $B - V$ color curve with those of normal and 91bg-like SNe Ia. One can see that the color curve of SN 2017fzw is very similar to that

Preprints (www.preprints.org) | NOT PEER-REVIEWED | Posted: 17 May 2023 doi:10.20944/preprints202305.1256.v1

of SN 2012ij in morphology, both are systematically much redder than those of normal SNe Ia. In particularly, SN 2017fzw tends to be even redder than all comparison SNe Ia after the reddest color. After $\sim +50$ days from the B-band maximum, all color curves became indistinguishable. On the other hand, the observed $B-V$ color of SN 2017fzw is significantly bluer than 91bg-like SNe Ia (i.e., $0.4-0.7$ mag [20]) at the B-band maximum light. It is also observed that SN 2017fzw reached the red peak earlier than normal SNe Ia.

The color stretch factor (S_{BV}) defined as $S_{BV} = t_{max}^{B-V}/30$ days [53], where t_{max}^{B-V} presents the peak time of the $B-V$ color curve, is proportional to t_{max}^{B-V}. Burns et al. (2014) [53] presented a relation between S_{BV} and $\Delta m_{15}(B)$ to estimate the factor S_{BV}, but found that the factor t_{max}^{B-V} was better than $\Delta m_{15}(B)$ in the case of fast-evolving 91bg-like SNe Ia. Thus, we utilize the former relation to calculate the S_{BV} of SN 2017fzw in this work, and obtain its $S_{BV} = 0.63$ with $t_{max}^{B-V} \approx 19$ days. The estimated S_{BV} is close to some transitional SNe Ia (e.g., ~ 0.65 for SN 1986G, [23,31]).

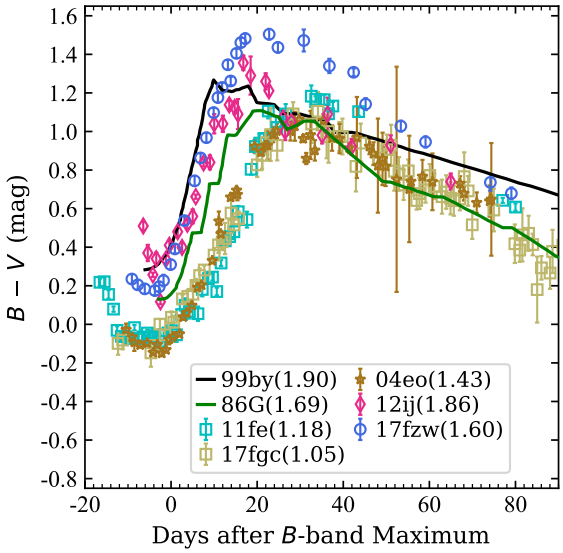

Figure 5. $B-V$ color curve of SN 2017fzw, and those of normal SNe 2011fe and 2017fgc, and transitional SNe 2004eo and 2012ij. All SNe Ia have been dereddened for the Milky Way and host galaxies.

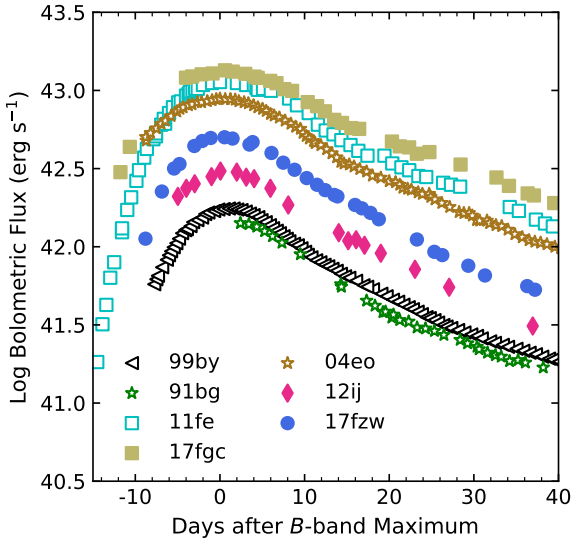

Figure 6. Quasi-bolometric (UV/optical) light curve of SN 2017fzwcompared with those of normal SNe 2011fe and 2017fgc (Zeng et al. 2021 [61]), and transitional SNe 2004eo and 2012ij (Li et al. 2022 [25]).

Preprints (www.preprints.org) | NOT PEER-REVIEWED | Posted: 17 May 2023 doi:10.20944/preprints202305.1256.v1

3.3. Bolometric Light Curves

According to response curves of different filters, the quasi-bolometric flux of SN 2017fzw was constructed by trapezoidal integration of flux densities in UV/optical ($UBVgri$) photometry, covering the emission range of 3000-9700 Å, as shown in Figure 6. Comparing its quasi-bolometric light curve with those of 91bg-like SNe 1991bg [16] and 1999by [14], transitional SNe 2004eo [59] and 2012ij [25], and normal SNe 2011fe [60] and 2017fgc [61], we find that SN 2017fzw most closely resembles SN 2012ij. Moreover, the modified radiation diffusion model of Arnett implemented in `Minim` Code [65–67] is employed to estimate the radioactive nickel mass of SN 2017fzw as $M_{Ni} = 0.18 \pm 0.03$ M$_\odot$. This is comparable to transitional SNe Ia within reasonable uncertainties (i.e., ~ 0.14 M$_\odot$, SN 1986G [31] and SN 2012ij [25]). We estimate a maximum luminosity of $L = (4.6 \pm 0.5) \times 10^{42}$ erg s^{-1}.

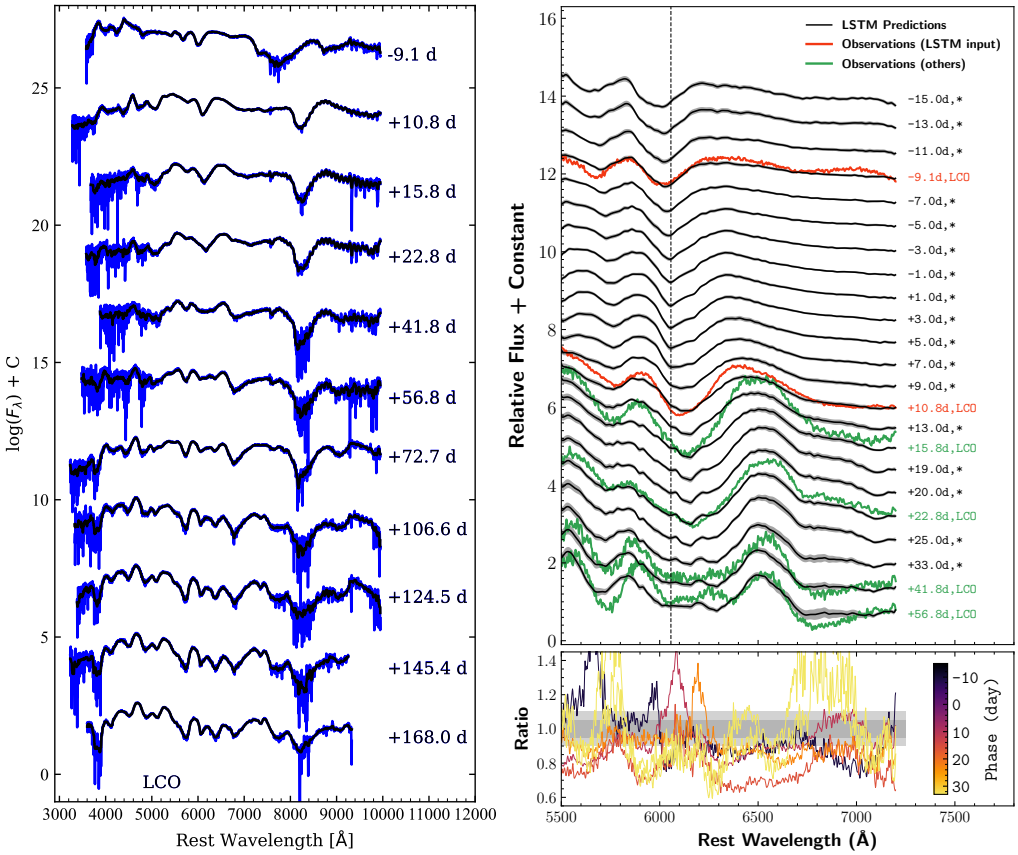

Figure 7. Left panel: observed (black curves) and smoothed (blue curves) spectra of SN 2017fzw obtained from LCO. The corresponding phases relative to its B-band maximum of this SN are marked on the right side. Right top panel: spectral sequence predicted from two spectra with phase difference ($\Delta p = 20$ days) using long short-term memory (LSTM) neural networks [68] for SN 2017fzw. The predictive mean spectra are marked by solid black curves, and their 2σ standard deviations are indicated by the gray shaded areas. The corresponding observed spectra are plotted as green curves, except for the two input spectra in red. The vertical dashed line indicates the Si II λ6355 absorption at -1.0 day. Right lower panel: flux ratios of predictions to observations for the spectral sequence. All spectra have been vertically shifted for better display.

4. Optical Spectroscopic Properties

Spectroscopic monitoring of SN 2017fzw are displayed in the left panel of Figure 7, spanning the period -9 to $+168$ days. The spectral evolution of SN 2017fzw is characterized by several key features found in 91bg-like SNe Ia discussed in the literature, of which we now further elaborate upon [56]. A spectrum of SN 2017fzw at pre-maximum light shows noticeable P-Cygni absorption features of IMEs, such as Si II, S II, Ca II and Mg II. Its

Preprints (www.preprints.org) | NOT PEER-REVIEWED | Posted: 17 May 2023 doi:10.20944/preprints202305.1256.v1

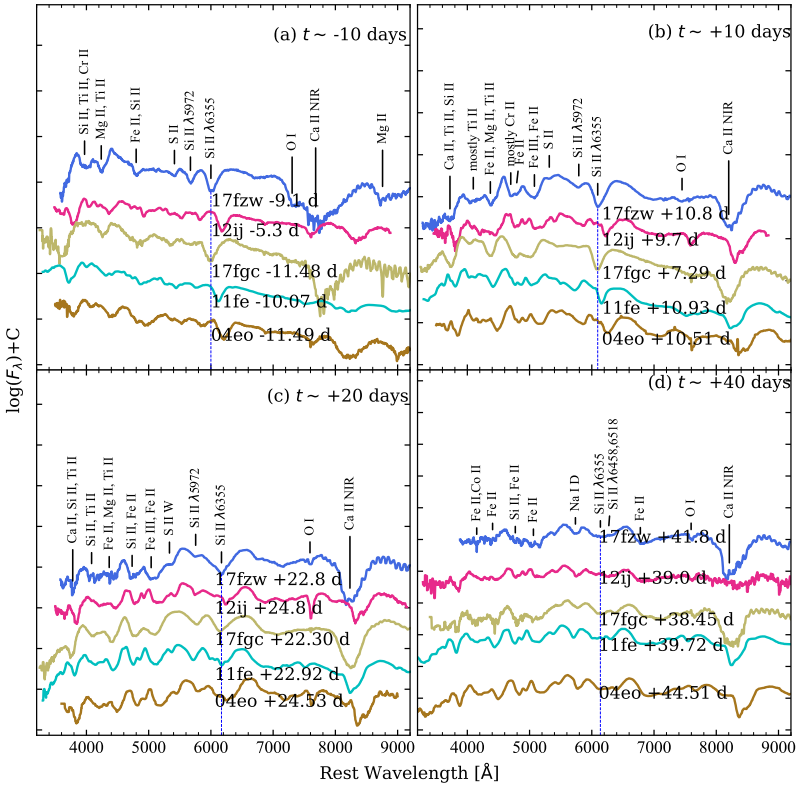

Figure 8. Optical spectra of SN 2017fzw at four different phases (i.e., −10d, +10d, +20d, and +40d) are compared with those of normal SNe 2011fe and 2017fgc, and transitional SNe 2004eo and 2012ij. All of the spectra have been corrected for redshift and reddening of host galaxies and the Milky Way, and shifted vertically for clarity.

spectra also has a prominent Ti II absorption feature, which is characteristic of 91bg-like SNe, confirming that SN 2017fzw belongs to the subluminous subclass. Moreover, the Si II λ5972 and O I absorption features of the SN 2017fzw spectra are found to be much stronger relative to normal SNe Ia at similar phases. After $\sim$ +10 days from the *B*-band maximum, the S II absorption features are nearly undetectable. In particular, the Si II λ5972 feature gradually becomes invisible after $\sim$ +20 days and is replaced by the Na I feature. However, the Si II λ6355 feature is still detectable up to about one month past *B*-band maximum light.

In Figure 8, detailed spectral comparisons among SN 2017fzw, normal SNe Ia, and transitional SNe Ia are displayed at four phases (i.e., −10d, +10d, +20d, and +40d). The comparison sample inlude SNe 2004eo [59], 2011fe [60], 2012ij [25], and 2017fgc [61]. Like SNe 2004eo and 2012ij, SN 2017fzw shows prominent Ti II and iron-group elements (IGE) absorption features after $\sim$ +10 days. One can see that SN 2017fzw is very similar to SN 2012ij in both overall shape and strength of characteristic spectral lines at each phase, except for Si II λ6355 and Ca II NIR absorption features. According to Li et al. (2022) [25], the spectra of SN 2012ij resemble those of SN 1999by. Thus, we could say that SN 2017fzw is similar to SN 1999by. These two different features in the spectra of SN 2017fzw tend to resemble SN 2017fgc, which is included in the high-velocity (HV) subgclass due to the classification criteria introduced by Wang et al. (2009) [69]. As shown in Figure 9, at later phases ($\sim$ +107 and +168 days) SN 2017fzw also tends to develop characteristics very similar to the HV SN 2017fgc. To summarize, the spectra of SN 2017fzw resembles the 91bg-like SNe Ia at early phases and evolves away from 91bg-like ones at later phases.

Preprints (www.preprints.org) | NOT PEER-REVIEWED | Posted: 17 May 2023 doi:10.20944/preprints202305.1256.v1

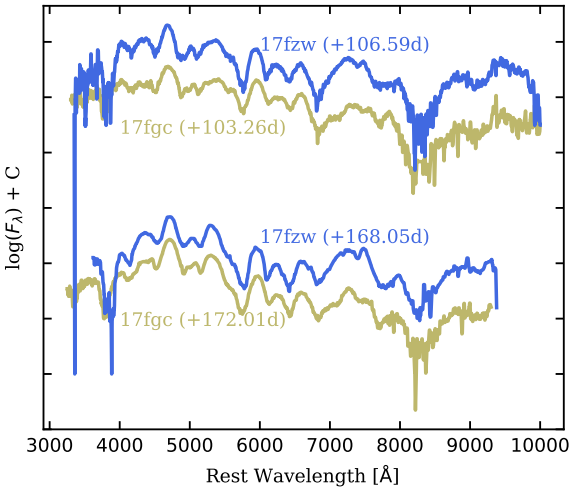

Figure 9. Comparison between spectra of SN 2017fzw (yellow curve) and SN 2017fgc (yellow curve) at around +105 and +170 days. As in Figure 8, both spectra have been corrected for redshift and reddening.

For SNe Ia, the velocity measured from Si II λ6355 at B-band maximum light is often used to determine their subclass [69]. Unfortunately, SN 2017fzw does not have optical spectral data at around B-band maximum light. Thus according to Hu et al. (2022), long short-term memory (LSTM) neural networks [68] is employed to predict the spectra of SN 2017fzw in this work, and results are shown in the right panel of Figure 7. One can see that the predictions of SN 2017fzw at around 6355 Å roughly coincide with its observations, except for its spectra after +23 days. For the predicted spectrum of SN 2017fzw at B-band maximum, its velocity of Si II λ6355 is measured as $v = 13,786 \pm 414$ km s^{-1}, significantly beyond the upper limit (i.e., $\sim$ 11800 km s^{-1} introduced by Wang et al. 2009 [69]) of the normal-velocity (NV) subclass. We thus classify SN 2017fzw as belonging to the HV subclass like SN 2017fgc. Consistent with the HV SNe Ia behaviour, the Ca II NIR absorption feature in the HV SNe 2017fgc and 2017fzw is much stronger than those of the NV SNe 2004eo, 2011fe, and 2012ij after one month past B-band maximum light [61].

5. Discussion

5.1. Transitional Photometric Properties

SN 2017fzw exhibits properties that are characteristic of transitional SNe Ia. Specifically, it has a fast decline rate with $\Delta m_{15}(B) = 1.60$ mag, and an earlier peak time in the i-band light curve compared to the B-band light curve [32]. Notably, this SN displays a significant shoulder/secondary maximum in r/i-band light curves, which distinguishes it from 91bg-like SNe Ia. Typically, normal SNe Ia have a stronger shoulder/secondary maximum in NIR light curves, which is associated with the recombination of IGE [70]. Taubenberger (2017) [64] suggested that fast-declining SNe Ia tend to display weaker and earlier shoulder/secondary maximum due to the earlier recombination of IGE. Furthermore, two NIR maxima may combine to form a delayed single NIR maximum in some 91bg-like SNe Ia. Transitional SNe Ia exhibit properties, including luminosity and temperature, that are intermediate to those of normal and 91bg-like SNe Ia. As such, it is reasonable to suggest that they have a weak shoulder/secondary maximum in their NIR light curves [25].

We estimate the B-band absolute peak magnitude (M^B_{max}) of SN 2017fzw to be approximately -17.77 mag, which is comparable to the brightness of 91bg-like SNe Ia (approximately -16.5 to -17.7 mag [64]). The $B - V$ color curve of SN 2017fzw is bluer than that of 91bg-like SNe Ia at B-band maximum, which is consistent with the findings of Taubenberger et al. (2008) [20]. They discovered that a SN Ia with $\Delta m_{15}(B) \leq 1.75$ mag has a relatively small luminosity, a double maximum in NIR light curves, and a rapid decay.

Preprints (www.preprints.org) | NOT PEER-REVIEWED | Posted: 17 May 2023 doi:10.20944/preprints202305.1256.v1

Figure 10 displays a comparison between $Mmax^B$ ($Mmax^B = -17.77$) of SN 2017fzw and color stretch factor ($S_{BV} = 0.63$, left panel) as well as Δm_{15} ($\Delta m_{15} = 1.60$,right panel), utilizing data from Krisciunas et al. (2017) [45] and Li et al. (2022) [25], encompassing overluminous SNe Ia, subluminous SNe Ia, transitional SNe Ia, and normal SNe Ia. It is evident that SN 2017fzw, along with several other SNe categorized as normal or subluminous, is located between the majority of the normal SNe Ia (right-pointing triangles) and the 91bg-like SN Ia (green square). This supports the hypothesis of a continuous distribution of SNe ranging from normal ($S_{BV} \leq\sim 0.5$) to 91bg-like ($S_{BV} \geq\sim 0.8$) [24]. This hypothesis implies that normal and 91bg-like SNe Ia may not originate from two entirely distinct populations.

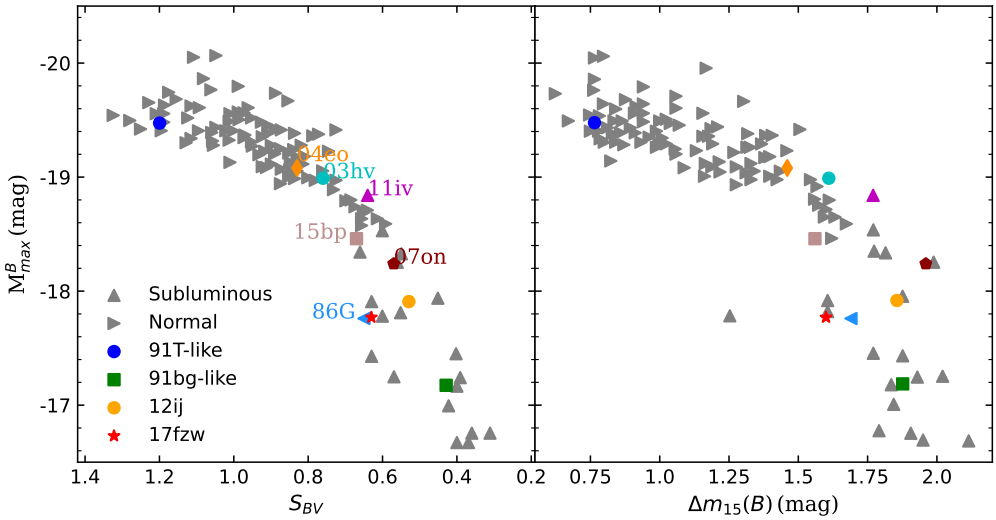

Figure 10. Left panel: M^B_{max} of SNe Ia versus their corresponding S_{BV}. Right panel: M^B_{max} of the same SNe Ia versus their corresponding $\Delta m_{15}(B)$. The sample includes SN 2017fzw (red star), transitional SN 2012ij (orange circle), 91T-like SN Ia (blue circle), 91bg-like SN Ia (green square), other subluminous SNe Ia, and normal SNe Ia. The sample is taken from Krisciunas et al. (2017) [45] and Li et al. (2022) [25].

5.2. Transitional Spectroscopic Properties

The spectral evolution of SN 2017fzw is analyzed and compared with normal and transitional SNe Ia in Figure 8 and 9. It is observed that its spectra shift from being more 91bg-like SNe (i.e., having a prominent Ti II absorption feature) at early phases to more normal SNe (mainly HV SN 2017fgc) at later phases, suggesting its transitional characteristics. Notably, SN 2017fzw belongs to the HV normal subclass according to the classification criteria of Wang et al. (2009) [69], which distinguishes it from most transitional SNe Ia (listed in Table 2). This can explain why SN 2017fzw, like HV SN Ia, exhibits a stronger Ca II NIR absorption feature and Si II λ6355 velocity compared to the SNe 2004eo and 2012ij.

For instance, Li et al. (2022) [25] discovered that transitional SN 2012ij falls into the NV subclass according to the same classification criteria established by Wang et al. (2009) [69]. This SN serves as a link between the NV subclass of the normal group and the 91bg-like SNe Ia. On the other hand, SN 2017fzw connects the HV subclass of the normal group with the 91bg-like SNe Ia, which further supports Li et al.'s (2022) [25] finding of a continuous distribution between normal SNe, including the NV and HV normal subclasses, and 91bg-like SNe Ia. Moreover, some authors have also identified a continuous distribution between normal and 91bg-like SNe Ia in other parameter spaces [22,71,72].

 doi:10.20944/preprints202305.1256.v1

Table 2. Photometric and spectroscopic properties of transitional SNe Ia.

name	S_{BV}	$\Delta m_{15}(B)$ (mag)	M^B_{max} (mag)	V ($\times 10^4$ km s^{-1})	SN Type	reference
SN 1986G	0.65	1.69	-17.76	0.81	NV	[23]
SN 2003hv	0.76	1.61	-18.99	-	LVG[1]	[73]
SN 2004eo	0.83	1.46	-19.08	1.07	NV	[59]
SN 2007on	0.57	1.96	-18.24	0.95	NV	[24]
SN 2011iv	0.63	1.77	-18.84	0.95	NV	[24]
SN 2012ij	0.53	1.86	-17.95	1.05	NV	[25]
SN 2015bp	0.67	1.56	-18.46	1.06	NV	[74]
SN 2017fzw	0.63	1.60	-17.77	1.38	HV	this paper

[1] Note that low-velocity gradient (LVG) subclass is proposed by Benetti et al. (2005) [75] base on the velocity gradient of the Si II λ6355, and most LVG SNe Ia belong to the NV subclass in general [61,69].

6. Conclusions

In this study, we presented and analyzed the photometric and spectroscopic data of the HV SN Ia 2017fzw with transitional properties. Our analysis revealed that SN 2017fzw has an M^B_{max} of -17.77 mag, which is close to the peak magnitude of 91bg-like SNe Ia. Based on its $\Delta m_{15}(B) = 1.60$ mag and color stretch factor ($S_{BV} = 0.63$), we identified SN 2017fzw as a transitional SN that bridges between normal and 91bg-like SNe, thus confirming its transitional nature. Additionally, we classified SN 2017fzw as belonging to the HV subclass with a velocity of $v = 13,786$ km s^{-1}. The spectra of SN 2017fzw show similarities to those of 91bg-like SNe, with prominent Ti II features at early phases, and gradually evolve to resemble normal SNe Ia (mainly HV subclass), with stronger Ca II NIR features at later phases.

In conclusion, our analysis shows that SN 2017fzw is a transitional SN Ia with properties that bridge the gap between normal and 91bg-like SNe Ia. This supports the hypothesis that there may be a continuous distribution of SNe spanning from normal to 91bg-like SNe, suggesting that these two groups may have a common origin. The discovery of transitional SN Ia provides an opportunity to investigate the relationships between these two groups, and to gain a better understanding of their progenitors and explosion mechanisms.

Author Contributions: Conceptualization, X.-Y.Z. and S.Z.; methodology, X.-Y.Z. and S.Z.; software, J.-Y.H., Y.-Y.L., X.-Y.Z. and S.Z.; validation, X.-Y.Z. and S.Z.; formal analysis, J.-Y.H. and Y.-Y.L.; investigation, J.-Y.H. and X.-Y.Z.; resources, S.Z. and X.-Y.Z.; data curation, A.Iskandar., K.A.Bostroem., D.A.Howell., C.McCully., and L.H.; writing—original draft preparation, J.-Y.H. and Y.-Y.L.; writing—review and editing, J.-Y.H., S.Z. and X.-Y.Z.; visualization, S.A.Bird., A.Esamdin., W.-X.L., T.-M.Z., J.-J.Z., S.-G.Z., Y.-S.X., Y.H. and L.-F.W.; All authors have read and agreed to the published version of the manuscript.

Funding: This research was funded by National Natural Science Foundation of China 12203029 and U2031202.

Institutional Review Board Statement: Not applicable.

Informed Consent Statement: Not applicable.

Data Availability Statement: The photometric and spectroscopic data analyzed for this study are downloaded from Las Cumbres Observatory (LCO) and *Neil Gehrels Swift Observatory* (*Swift*).

Acknowledgments: The authors thank the staffs of LCO network 1-m/2-m telescopes and *Swift* that obsevred and provided the data. And the LCO group is supported by NSF grants AST-1911225, AST-1911151, and NASA grant 80NSSC19K1639. And this work is supported by The National Natural Science Foundation of China (NSFC, grants 11803076), and the High Level Talent–Heaven Lake Program of Xinjiang Uygur Autonomous Region of China.

Conflicts of Interest: The authors declare no conflict of interest.

 doi:10.20944/preprints202305.1256.v1

Appendix A

Table A1. UV and optical photometry of SN 2017fzw obtained from LCO telescopes and SWIFT.

MJD [1]	U	B	V	g	r	i	$UVW2$	$UVW1$
57974.36	···	···	···	···	17.169(0.009[2])	···	···	···
57978.02	16.475(0.054)	15.784(0.029)	15.578(0.045)	···	···	···	18.338(0.090)	17.890(0.162)
57981.81	···	15.359(0.025)	15.124(0.024)	15.212(0.023)	···	···	···	···
57980.17	···	14.982(0.025)	14.776(0.025)	14.853(0.021)	14.611(0.025)	15.144(0.026)	···	···
57980.76	15.599(0.065)	14.973(0.037)	14.716(0.055)	···	···	···	17.910(0.182)	17.079(0.058)
⋮	⋮	⋮	⋮	⋮	⋮	⋮	⋮	⋮
58156.61	···	···	···	18.990(0.045)	···	···	···	···
58167.54	···	19.389(0.042)	19.429(0.057)	19.178(0.031)	19.852(0.068)	···	···	···
58193.51	···	···	···	19.725(0.046)	···	···	···	···
58215.06	···	···	···	20.105(0.041)	···	···	···	···
58226.39	···	20.449(0.078)	···	···	···	···	···	···

[1] Phases are relative to the epoch of B-band maximum brightness (MJD = 57987.90).

[2] Uncertainties, in units of 0.001 mag, are 1σ.

Note. Measurements are calibrated to the AB magnitude system. (This table is available in its entirety in machine-readable form.)

References

1. Howell, D.A. Type Ia supernovae as stellar endpoints and cosmological tools. *NatCo* **2011**, *2*, 350–375.
2. Riess, A.G.; Filippenko A.V.; Challis, P.; et al. Observational Evidence from Supernovae for an Accelerating Universe and a Cosmological Constant. *AJ* **1998**, *116*, 1009–1038.
3. Hoyle, F; Fowler, W.A. Nucleosynthesis in Supernovae. *ApJ* **1960**, *132*, 565–590.
4. Whelan, J.; Iben, I. Binaries and Supernovae of Type I. *Sci* **1973**, *186*, 1007–1014.
5. Podsiadlowski, P.; Mazzali, P.; Lesaffre, P.; Han, Z.; Förster, F. The nuclea r diversity of Type Ia supernova explosions. *NewAR* **2008**, *52*, 381–385.
6. Iben, I.; Tutukov, A.V. Supernovae of type I as end products of the evolution of binaries with components of moderate initial mass. *ApJS* **1984**, *54*, 335–372.
7. Wang, X.; Wang, L.; Filippenko, A.V.; Zhang, T.; Zhao, X. Evidence for Two Distinct Populations of Type Ia Supernovae. *Sci* **2013**, *340*, 170–173.
8. Wang, B. Mass-accreting white dwarfs and type Ia supernovae. *RAA* **2018**, *18*, 049.
9. Branch, D.; Fisher, A.; Nugent, P. On the Relative Frequencies of Spectroscopically Normal and Peculiar Type IA Supernovae. *AJ* **1993**, *106*, 2383–2391.
10. Filippenko, A.V. Optical Spectra of Supernovae. *ARA&A* **1997**, *35*, 309–355.
11. Filippenko, A.V.; Richmond, M.W.; Matheson, T.; et al. The Peculiar Type IA SN 1991T: Detonation of a White Dwarf? *ApJL* **1992**, *384*, L15–L18.
12. Phillips, M.M.; Wells, L.A.; Suntzeff, N.B.; et al. SN 1991T: Further Evidence of the Heterogeneous Nature of Type IA Supernovae. *AJ* **1992**, *103*, 1632–1637.
13. Ruiz-Lapuente, P.; Cappellaro, E.; Turatto, M.; et al. Modeling the Iron-dominated Spectra of the Type IA Supernova SN 1991T at Premaximum. *ApJL* **1992**, *387*, L33–L36.
14. Garnavich, P.M.; Bonanos, A.Z.; Krisciunas, K.; et al. The Luminosity of SN 1999by in NGC 2841 and the Nature of "Peculiar" Type Ia Supernovae. *ApJ* **2004**, *613*, 1120–1132.
15. Filippenko, A.V.; Richmond, M.W.; Branch, D.; et al. The Subluminous, Spectroscopically Peculiar Type 1a Supernova 1991bg in the Elliptical Galaxy NGC 4374. *AJ* **1992**, *104*, 1543–1556.
16. Filippenko, A.V.; Kirshner, R.P.; Phillips, M.M.; et al. SN 1991bg: A Type IA Supernova With a Difference. *AJ* **1993**, *105*, 301–313.
17. Howell, D.A. The Progenitors of Subluminous Type Ia Supernovae. *ApJL* **2001**, *554*, L193–L196.
18. Li, W.; Leaman, J.; Chornock, R.; et al. Nearby supernova rates from the Lick Observatory Supernova Search - II. The observed luminosity functions and fractions of supernovae in a complete sample. *MNRAS* **2011**, *412*, 1441–1472.
19. Srivastav, S.; Anupama, G.C.; Sahu, D.K.; Ravikumar, C.D. SN 2015bp: adding to the growing population of transitional Type Ia supernovae. *MNRAS* **2017**, *466*, 2436–2449.
20. Taubenberger, S.; et al. The underluminous Type Ia supernova 2005bl and the class of objects similar to SN 1991bg. *MNRAS* **2008**, *385*, 75–96.
21. Dhawan, S.; Leibundgut, B.; Spyromilio, J.; Blondin, S. Two classes of fast-declining Type Ia supernovae. *A&A* **2017**, *602*, A118.

22. González-Gaitán, S.; Perrett, K.; Sullivan, M.; et al. Subluminous Type Ia Supernovae at High Redshift from the Supernova Legacy Survey. *ApJ* **2011**, *727*, 107.
23. Phillips, M.M.; Phillips, A.C.; Heathcote, S.R.; et al. The type IA supernova 1986G in NGC 5128 : optical photometry and spectra. *PASP* **1987**, *99*, 592–605.
24. Gall, C.; Stritzinger, M.D.; Ashall, C.; et al. Two transitional type Ia supernovae located in the Fornax cluster member NGC 1404: SN 2007on and SN 2011iv. *A&A* **2018**, *611*, A58.
25. Li, Z.; Zhang, T.; Wang, X.; et al. SN 2012ij: A Low-luminosity Type Ia Supernova and Evidence for a Continuous Distribution from a 91bg-like Explosion to Normal Ones. *ApJ* **2022**, *927*, 142.
26. Moon, D.S.; Ni, Y.Q.; Drout, M.R.; et al. Rapidly Declining Hostless Type Ia Supernova KSP-OT-201509b from the KMTNet Supernova Program: Transitional Nature and Constraint on ^{56}Ni Distribution and Progenitor Type. *ApJ* **2021**, *910*, 151.
27. Phillips, M.M. The Absolute Magnitudes of Type IA Supernovae. *ApJL* **1993**, *413*, L105–L108.
28. Phillips, M.M.; Lira, P.; Suntzeff, N.B.; et al. The Reddening-Free Decline Rate Versus Luminosity Relationship for Type IA Supernovae. *AJ* **1999**, *118*, 1766–1776.
29. Ashall, C.; Mazzali, P.A.; Sasdelli, M.; Prentice, S.J. Luminosity distributions of Type Ia supernovae. *MNRAS* **2016a**, *460*, 3529–3544.
30. Prieto, J.L.; Rest, A.; Suntzeff, N.B. A New Method to Calibrate the Magnitudes of Type Ia Supernovae at Maximum Light. *ApJ* **2006**, *647*, 501–512.
31. Ashall, C.; Mazzali, P.A.; Pian, E.; James, P.A. Abundance stratification in Type Ia supernovae - V. SN 1986G bridging the gap between normal and subluminous SNe Ia. *MNRAS* **2016b**, *463*, 1891–1906.
32. Hsiao, E.Y.; Burns, C.R.; Contreras, C.; et al. Strong near-infrared carbon in the Type Ia supernova iPTF13ebh. *A&A* **2015**, *578*, A9.
33. Tartaglia, L.; Sand, D.J.; Valenti, S.; et al. The Early Detection and Follow-up of the Highly Obscured Type II Supernova 2016ija/DLT16am. *ApJ* **2018**, *853*, 62.
34. Valenti, S.; Sand, D.J.; Tartaglia, L. DLT40 Transient Discovery Report for 2017-08-09. *TNSTR* **2017**, *855*, 1.
35. Tartaglia, L.; Sand, D.J.; Wyatt, S.; et al. The discovery of DLT17cd/AT 2017fzw with PROMPT. *The Astronomer's Telegram* **2017**, *10629*, 1.
36. Hosseinzadeh, G.; Valenti, S.; Howell, D.A.; Arcavi, I.; Mccully, C. Global SN Project Transient Classification Report for 2017-08-13. *TNSCR* **2017**, *865*, 1.
37. Mould, J.R.; Huchra, J.P.; Freedman, W.L.; et al. The Hubble Space Telescope Key Project on the Extragalactic Distance Scale. XXVIII. Combining the Constraints on the Hubble Constant. *ApJ* **2000**, *529*, 786–794.
38. NASA/IPAC Extragalactic Database (NED). Available online: https://ned.ipac.caltech.edu (14 09 2022).
39. Brown, T.M.; Burleson, B.; Crellin, M.; et al. Las Cumbres Observatory Global Telescope 1-meter Telescope Project: Design, Deployment Plans, Status. *AAS* **2010**, *215*, 441.06.
40. Brown, T.M.; Baliber, N.; Bianco, F.B.; et al. Las Cumbres Observatory Global Telescope Network. *PASP* **2013**, *125*, 1031–1055.
41. Howell, D.A.; Global Supernova Project. The Global Supernova Project. *AAS* **2017**, *230*, 318.03.
42. Valenti, S.; Baliber, N.; Bianco, F.B.; et al. The diversity of Type II supernova versus the similarity in their progenitors. *MNRAS* **2016**, *459*, 3939–3962.
43. Landolt, A.U. Broadband UBVRI Photometry of the Baldwin-Stone Southern Hemisphere Spectrophotometric Standards. *AJ* **1992**, *104*, 372–376.
44. Smith, A.J.; Tucker, D.L.; Kent, S.; et al. The u'g'r'i'z' Standard-Star System. *AJ* **2002**, *123*, 2121–2144.
45. Krisciunas, K.; Contreras, C.; Burns, C.R.; et al. The Carnegie Supernova Project. I. Third Photometry Data Release of Low-redshift Type Ia Supernovae and Other White Dwarf Explosions. *AJ* **2017**, *154*, 211.
46. Phillips, M.M.; Contreras, C.; Hsiao, E.Y.; et al. Carnegie Supernova Project-II: Extending the Near-infrared Hubble Diagram for Type Ia Supernovae to z $\sim$ 0.1. *PASP* **2019**, *131*, 014001.
47. Gehrels, N.; Chincarini, G.; Giommi, P.; et al. The Swift Gamma-Ray Burst Mission. *ApJ* **2004**, *611*, 1005–1020.
48. Roming, P.W.A.; Kennedy, T.E.; Mason, K.O.; et al. The Swift Ultra-Violet/Optical Telescope. *SSRv* **2005**, *120*, 95–142.
49. Breeveld, A.A.; Landsman, W.; Holland, S.T.; et al. An Updated Ultraviolet Calibration for the Swift/UVOT. *AIPC* **2011**, *1358*, 373–376.
50. Brown, P.J.; Breeveld, A.A.; Holland, S.T.; Kuin, P.; Pritchard, T. SOUSA: the Swift Optical/Ultraviolet Supernova Archive. *AP&SS* **2014**, *354*, 89–96.
51. Sand, D.J.; Brown, T.; Haynes, R.; Dubberley, M. Floyds: A Robotic Spectrograph for the Faulkes Telescopes. *AAS* **2011**, *218*, 132.03.
52. Burns, C.R.; Stritzinger, M.; Phillips, M.M.; et al. The Carnegie Supernova Project: Light-curve Fitting with SNooPy. *AJ* **2011**, *141*, 19.
53. Burns, C.R.; Stritzinger, M.; Phillips, M.M.; et al. The Carnegie Supernova Project: Intrinsic Colors of Type Ia Supernovae. *ApJ* **2014**, *789*, 32.
54. Riess, A.G.; Filippenko, A.V.; Li, W.; Schmidt, B.P. The Rise Time of Nearby Type IA Supernovae. *AJ* **1999**, *118*, 2675–2688.
55. Zheng, W.; Kelly, P.L.; Filippenko, A.V. An Empirical Fitting Method for Type Ia Supernova Light Curves. II. Estimating the First-light Time and Rise Time. *ApJ* **2017**, *848*, 66.

56. Graham, M.L.; Kennedy, T.D.; Kumar, S.; et al. Nebular-phase spectra of Type Ia supernovae from the Las Cumbres Observatory Global Supernova Project. *MNRAS* **2022**, *511*, 3682–3707.
57. Hough, J.H.; Bailey, J.A.; Rouse, M.F.; Whittet, D.C.B. Interstellar polarization in the dust lane of Centaurus A (NGC 5128). *MNRAS* **1987**, *227*, 1p–5p.
58. Ganeshalingam, M.; Li, W.; Filippenko, A.V.; et al. Results of the Lick Observatory Supernova Search Follow-up Photometry Program: BVRI Light Curves of 165 Type Ia Supernovae. *ApJS* **2010**, *190*, 418–448.
59. Pastorello, A.; Mazzali, P.A.; Pignata, G.; et al. ESC and KAIT observations of the transitional Type Ia SN 2004eo. *MNRAS* **2007**, *377*, 1531–1552.
60. Zhang, K.; Wang, X.; Zhang, J.; et al. Optical Observations of the Type Ia Supernova SN 2011fe in M101 for Nearly 500 Days. *ApJ* **2016**, *820*, 67.
61. Zeng, X.; Wang, X.; Esamdin, A.; et al. SN 2017fgc: A Fast-expanding Type Ia Supernova Exploded in Massive Shell Galaxy NGC 474. *ApJ* **2021**, *919*, 49.
62. Schlafly, E.F.; Finkbeiner, D.P. Measuring Reddening with Sloan Digital Sky Survey Stellar Spectra and Recalibrating SFD. *ApJ* **2011**, *737*, 103.
63. Cardelli, J.A.; Clayton, G.C.; Mathis, J.S. The Relationship between Infrared, Optical, and Ultraviolet Extinction. *ApJ* **1989**, *345*, 245–256.
64. Taubenberger, S. The Extremes of Thermonuclear Supernovae. In *Handbook of Supernovae*; Alsabti, A.W., Murdin, P.; Springer International Publishing AG: Berlin, German, 2017; pp. 317–373.
65. Arnett, W.D. Type I supernovae. I - Analytic solutions for the early part of the light curve. *ApJ* **1982**, *253*, 785–797.
66. Chatzopoulos, E.; Wheeler, J.C.; Vinko, J. Generalized Semi-analytical Models of Supernova Light Curves. *ApJ* **2012**, *746*, 121.
67. Li, W.; Wang, X.; Vinkó, J.; et al. Photometric and Spectroscopic Properties of Type Ia Supernova 2018oh with Early Excess Emission from the Kepler 2 Observations. *ApJ* **2019**, *870*, 12.
68. Hu, L.; Chen, X.; Wang, L. Spectroscopic Studies of Type Ia Supernovae Using LSTM Neural Networks. *ApJ* **2022**, *930*, 70.
69. Wang, X.; Filippenko, A.V.; Ganeshalingam, M.; et al. Improved Distances to Type Ia Supernovae with Two Spectroscopic Subclasses. *ApJ* **2009**, *699*, L139–L143.
70. Kasen, D. Secondary Maximum in the Near-Infrared Light Curves of Type Ia Supernovae. *ApJ* **2006**, *649*, 939–953.
71. Blondin, S.; Matheson, T.; Kirshner, R.P.; et al. The Spectroscopic Diversity of Type Ia Supernovae. *AJ* **2012**, *143*, 126.
72. Burns, C.R.; Parent, E.; Phillips, M.M.; et al. The Carnegie Supernova Project: Absolute Calibration and the Hubble Constant. *ApJ* **2018**, *869*, 56.
73. Leloudas, G.; Stritzinger, M.D.; Sollerman, J.; et al. The normal Type Ia SN 2003hv out to very late phases. *A&A* **2009**, *505*, 265–279.
74. Wyatt, S.D.; Sand, D.J.; Hsiao, E.Y.; et al. Strong Near-infrared Carbon Absorption in the Transitional Type Ia SN 2015bp. *ApJ* **2021**, *914*, 57.
75. Benetti, S; Cappellaro, E.; Mazzali, P.A.; et al. The Diversity of Type Ia Supernovae: Evidence for Systematics?. *ApJ* **2005**, *623*, 1011–1016.